

pubs.acs.org/ac Article

# Quantitative Separation of Unknown Organic-Metal Complexes by Liquid Chromatography-Inductively Coupled Plasma-Mass Spectrometry

Christian Dewey, Daniel I. Kaplan, Scott Fendorf, and Rene M. Boiteau\*



Cite This: Anal. Chem. 2023, 95, 7960-7967



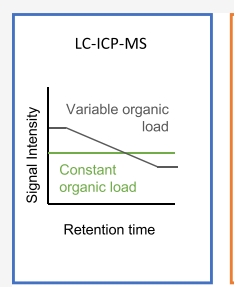
**ACCESS** I

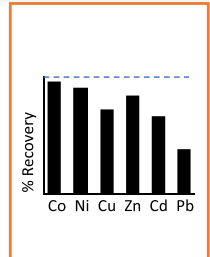
Metrics & More

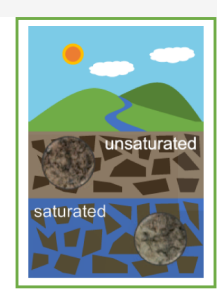
Article Recommendations

Supporting Information

ABSTRACT: Dissolved organic matter (DOM) is widely recognized to control the solubility and reactivity of trace metals in the environment. However, the mechanisms that govern metal-DOM complexation remain elusive, primarily due to the analytical challenge of fractionating and quantifying metal—organic species within the complex mixture of organic compounds that comprise DOM. Here, we describe a quantitative method for fractionation and element-specific detection of organic—metal complexes using liquid chromatography with online inductively coupled plasma mass spectrometry (LC—ICP-MS). The method implements a post-column compensation gradient to stabilize ICP—MS elemental response across the LC solvent gradient, thereby







Eliminate matrix effects on quantitation

Assess metal recovery

Survey environmental metal speciation

overcoming a major barrier to achieving quantitative accuracy with LC-ICP-MS. With external calibration and internal standard correction, the method yields concentrations of organic-metal complexes that were consistently within 6% of their true values, regardless of the complex's elution time. We used the method to evaluate the effects of four stationary phases (C18, phenyl, amide, and pentafluoroylphenyl propyl) on the recovery and separation of environmentally relevant trace metals (Mn, Fe, Co, Ni, Cu, Zn, Cd, and Pb) in Suwannee River Fulvic Acid and Suwannee River Natural Organic Matter. The C18, amide, and phenyl phases generally yielded optimal metal recoveries (>75% for all metals except Pb), with the phenyl phase separating polar species to a greater extent than C18 or amide. We also fractionated organic-bound Fe, Cu, and Ni in oxidized and reduced soils, revealing divergent metal-DOM speciation across soil redox environments. By enabling quantitative fractionation of DOM-bound metals, our method offers a means for advancing a mechanistic understanding of metal-organic complexation throughout the environments.

# **■ INTRODUCTION**

Dissolved organic matter (DOM) is widely recognized to control the solubility, reactivity, and bioavailability of trace metals in soil and aquatic systems. Organic ligands within DOM bind to a vast array of trace metals, including Fe, Co, Ni, Cu, Zn, Cd, and Pb, thereby stabilizing dissolved metals across a range of concentrations—from picomolar levels of Fe and Zn in the ocean (where they are limiting nutrients) to micromolar levels of Cu and Cd in polluted watersheds.<sup>1,2</sup> However, despite the centrality of organic complexation to a plethora of trace metal biogeochemical cycles, the mechanisms that govern the metal-binding properties of DOM remain poorly constrained.<sup>3,4</sup> A heterogeneous mixture of metabolites and decaying detritus, DOM contains an assortment of metal ligands, including specific biomolecules synthesized by microbes, fungi, and plants for metal uptake or detoxification, as well as organic byproducts of biomass degradation with diverse metal-binding functional groups, each with distinct metal selectivity and affinity.3,5 Resolving distinct fractions of DOM and measuring the concentrations of metals bound to those fractions remains a major analytical challenge—one

which limits our understanding of the selectivity and affinity of DOM for trace metal cations and therefore of trace metal solubility and reactivity in environmental systems. Overcoming this challenge requires quantitative methods that can detect multiple metals bound to compounds within chemically distinct fractions of complex organic mixtures.

Previous investigations of metal complexation by DOM have employed electrochemical techniques (potentiometry and voltammetry) to quantify and operationally define the aggregate metal-binding properties of DOM.<sup>2,3,6,7</sup> Electrochemical studies show that DOM stabilizes dissolved metal concentrations above the solubility of inorganic forms; these methods are the basis for numerical models of metal speciation, which assume that metal binding only occurs at

Received: February 15, 2023 Accepted: April 23, 2023 Published: May 10, 2023





carboxylic and phenolic sites. <sup>8–10</sup> However, there is increasing evidence that low-abundance binding sites with high metal specificity and affinity, such as amide, phosphoryl, and thiol groups, <sup>6,11,12</sup> as well as multidentate and mixed coordination binding sites, may overshadow carboxyl and phenolic groups in controlling the speciation—and therefore reactivity and solubility—of organic-bound trace metals in the environment. <sup>2,13–18</sup> It is critical to incorporate these mechanisms into organic—metal speciation models to better predict trace metal cycles in the environment, yet doing so requires analytical methods that can resolve chemically distinct DOM fractions and quantify their selectivity and affinity for multiple trace metals.

Reverse phase liquid chromatography (LC) with online inductively coupled plasma mass spectrometry (ICP-MS) offers a sensitive approach for the quantitative detection of metals within DOM fractions. While LC-ICP-MS has been previously used to quantify specific organic-metal complexes in marine and terrestrial environments, <sup>19–22</sup> its use for quantitative multi-element detection has been limited by variation in ICP-MS elemental response during the chromatographic separation.<sup>23</sup> Several approaches have been developed to address this issue for single element analyses, including internal standard correction; 20 use of a standard curve for target species; 19,24-27 isotope dilution for elements with multiple isotopes; 28-32 and implementation of a post-column compensation gradient. 30,33,34 However, no method currently exists for quantitative LC-ICP-MS analyses of multiple DOMbound metals. Furthermore, the effects of chromatographic stationary phase on the separation and recovery of metal-DOM complexes are largely unknown. Partitioning of metal ions from DOM to the stationary phase, and subsequent loss of metals from the DOM sample, or conversely, complexation by DOM of metals contained in the column housing or particles (and thus contamination of the DOM sample with metal ions) both may introduce substantial quantitative error during LC-ICP-MS measurements.

Here, we developed a novel LC–ICP-MS method which significantly advances the use of a compensation gradient to accurately quantify multiple metals within chemically distinct fractions of DOM. We also developed a novel computer application, which is freely available, to facilitate a streamlined workflow for multielement quantitation and calibration of LC–ICP-MS data. Using the method and the computer application, we elucidated the effects of four stationary phases (C18, amide, HS F5, and phenyl) on the recovery and separation of DOM-bound metals. Finally, we used the method to detect and quantify dissolved trace metals within equivalent (LC-separated) fractions of DOM along a soil redox gradient, revealing differences in trace metal speciation that would be undetected by electrochemical methods.

# **■** METHODS

Materials, Standards, and Reagents. Ultrahigh purity water (18.2 M $\Omega$  cm), trace-metal grade nitric acid, and Optima-grade methanol (MeOH), ammonium hydroxide (NH<sub>4</sub>OH), ammonium formate (Fisher Scientific) were used throughout this study. Suwannee River Natural Organic Matter (SRNOM) and Suwannee River Fulvic Acid (SRFA) were purchased from the International Humic Substances Society. Solutions of 0.75  $\mu$ M cyanocobalamin, ferrioxamine E, and ferrochrome were prepared in ultrahigh purity water. Single-element ICP–MS standards (Inorganic Ventures) were used

to prepare calibration standards for Mn, Fe, Co, Ni, Cu, Zn, Cd, and Pb at 25, 50, 100, and 200 ppb in 1% nitric acid, as well as an internal standard solution of 4 ppb In in 1% nitric acid.

Solutions of SRNOM and SRFA were prepared in ultrapure water at a concentration of 200 mg DOM/L (100 mg DOC/ L). This concentration falls within the range of environmentally relevant DOC concentrations  $(0-100 \text{ mg DOC/L})^{35}$ and, further, is representative of DOM concentrations obtained after purification and desalting of environmental samples. From each DOM solution, four samples were prepared: (1) unamended DOM; (2) DOM amended with Co, Ni, Cu, Zn, Cd (8  $\mu$ M), and Pb (4  $\mu$ M); (3) DOM amended with Co, Ni, Cu, Zn, and Cd (16  $\mu$ M) and Pb (8  $\mu$ M); and (4) DOM amended with a dilute nitric acid solution. Each sample was also amended with cyanocobalamin (to 0.5  $\mu$ M), and pH was adjusted to 5.5 using NH<sub>4</sub>OH. Metals were added to SRNOM and SRFA in a dilute nitric acid solution to ensure that all metals were added in a dissolved form. After adjustment of the sample pH to 5.5, >97% of all metals was predicted by the NICA-Donnan model to be complexed by DOM. The amendment volumes and concentrations for the sample solutions are shown in Table S1, and sample preparation is described in the Supporting Information. Predicted metal speciation is shown in Table S2.

Soil samples were collected from partially dry and fully saturated soil horizons within the Tims Branch floodplain (33.33762 N, 81.71830 W) at the Savannah River Site (Aiken, SC, USA). Differences in texture and color were indicative of contrasting redox conditions between the samples. A detailed description of sample collection and DOM extraction can be found in the Supporting Information

High-Performance Liquid Chromatography. Chromatographic separations were performed with a biocompatible HPLC system (Thermo Scientific UltiMate 3000), which was equipped with titanium and polyether-ether-ketone (PEEK) fittings and tubing to reduce background concentrations of metals and to limit partitioning of the sample to surfaces within the system. Separations were performed with either a quaternary gradient pump (for the SRNOM and SRFA samples) or a binary capillary pump (for the soil DOM samples). Prior to being routed to the ICP-MS, the column eluent passed through a variable wavelength detector measuring UV absorbance at 254 nm. Mobile phases (ultrahigh purity water and Optima-grade MeOH) were buffered with 5 mM ammonium formate and were prepared in fluorinated ethylene propylene (FEP) bottles. A second HPLC pump delivered a post-column compensation gradient, which oppositely mirrored the separation gradient, resulting in a constant flux of MeOH to the ICP-MS. The second pump also supplied an internal standard solution (4 ppb In in 1% nitric acid, prepared in a FEP bottle). The compensation gradient and internal standard were continuously mixed with the column eluent before the conjoined flow entered the ICP-MS. A schematic of the instrument configuration is shown in Figure S1.

The SRNOM and SRFA samples were separated on C18, phenyl, HS F5, and amide reversed phased columns (Supelco Ascentis;  $20 \times 4$  mm,  $5 \mu$ m). We chose these columns because they represent a range of functional chemistries and retention mechanisms, including octadecyl alkane groups and hydrophobic and van der Waals interactions (C18); phenyl groups and pi-pi interactions (phenyl); pentafluorophenyl propyl

groups and electrophilic bonding (HS F5); and amide groups and hydrogen bonding (amide). Sample volumes of 50 µL were injected at a flow rate of 200  $\mu$ L/min, and a 10 min linear gradient was run from 95% H<sub>2</sub>O, 5% MeOH to 5% H<sub>2</sub>O, 95% MeOH, followed by a 1 min isocratic elution with 5% H<sub>2</sub>O, 95% MeOH and an 8 min re-equilibration at 95% H<sub>2</sub>O, 5% MeOH. The pump delivering the compensation gradient and the internal standard solution operated at a total flow rate of 500  $\mu$ L/min, with the internal standard continuously comprising 60% of total flow. The compensation gradient consisted of a 10 min linear ramp from 2% H<sub>2</sub>O, 38% MeOH to 38% H<sub>2</sub>O, 2% MeOH, followed by a 1 min isocratic elution with 38% H<sub>2</sub>O, 2% MeOH and 8 min hold at 2% H<sub>2</sub>O, 38% MeOH. Between the separation pump and the compensation/ internal standard pump, the ICP-MS continuously received 200  $\mu$ L/min MeOH, 200  $\mu$ L/min H<sub>2</sub>O, and 300  $\mu$ L/min 4 ppb In in 1% HNO<sub>3</sub> during the SRNOM and SRFA separations. Soil DOM was separated with a glass lined C18 micro column (ZORBAX Eclipse XDB; Agilent; 0.5 × 150 mm, 3.5  $\mu$ m) at a flow rate of 40  $\mu$ L/min. Details of the soil DOM separations are described in the Supporting Information. LC operating conditions are listed in Table S3.

Calibration standards were measured by injecting a blank solution (1% HNO<sub>3</sub>) and four standard solutions (25, 50, 100, and 200 ppb in 1% HNO<sub>3</sub>) of Mn, Fe, Co, Ni, Cu, Zn, Cd, and Pb through a titanium zero dead volume connector in the place of a separation column. Effluent was conjoined with the flow from the compensation pump, and the combined flow was delivered to the ICP–MS. The separation pump and the compensation pump operated for 1 min at the initial isocratic conditions used in the separations while metal signal intensity was measured. Linear regression of the standard concentrations and the blank-subtracted peak areas of the standards were used to derive a calibration curve. A new calibration curve was measured at the start of each run and after 48 h of continuous operation of the system.

ICP-MS Instrumentation. Measurements of <sup>55</sup>Mn, <sup>56</sup>Fe, <sup>59</sup>Co, <sup>60</sup>Ni, <sup>63</sup>Cu, <sup>66</sup>Zn, <sup>111</sup>Cd, <sup>115</sup>In, and <sup>208</sup>Pb were performed with a single quadrupole ICP-MS instrument (iCAP RQ; ThermoFisher Scientific) equipped with Pt skimmer and sample cones. To minimize polyatomic interferences, the instrument was run in kinetic energy discrimination mode using a hexapole collision cell with He collision gas. Oxygen gas was introduced at a flow rate of 25 mL/min to enhance combustion of organic solvent and prevent carbon build up on the cones. The spray chamber was maintained at -5 °C to reduce the organic solvent load to the plasma. The instrument was tuned daily with a commercially available tuning solution (ThermoFisher Scientific) in 2% HNO<sub>3</sub> by free aspiration with PTFE tubing. ICP-MS operating conditions are listed in Table S4.

**Data Analysis.** We developed a Python-based computer application to process and analyze LC-ICP-MS data. The application includes a graphical user interface through which the user can generate calibration curves, perform an internal standard correction, and calculate concentrations of metals within distinct DOM fractions. The application is open-source and available on GitHub (https://github.com/boiteaulab/LCICPMS-ui).

### RESULTS AND DISCUSSION

Standardization of ICP-MS Elemental Response. Unaddressed, the variation in ICP-MS elemental response

during the LC solvent gradient severely limits the quantitative accuracy of LC–ICP-MS analyses, particularly for unknown complexes of multiple metals. The effects of the LC solvent gradient on ICP–MS elemental response are shown in Figure 1a, which display the <sup>115</sup>In signal intensity of the internal

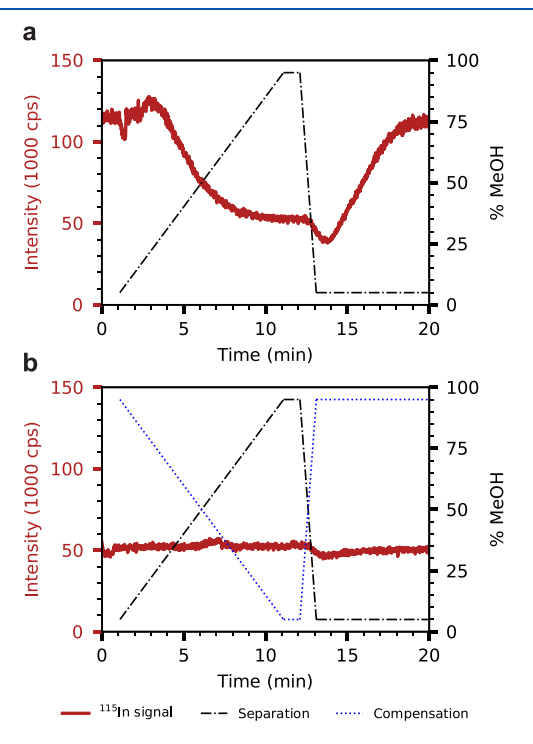


**Figure 1.** (a) Effects of solvent composition on ICP–MS signal intensity. As the organic solvent load increases during a reversed-phase separation, <sup>115</sup>In signal intensity decreases due to cooling of the plasma and changes in nebulization of the sample. (b) The compensation gradient, which is mixed with the separation eluent before the conjoined flow is routed to the ICP–MS, yields isocratic solvent conditions at the ICP–MS, resulting in stable <sup>115</sup>In signal intensity throughout the separation.

standard during a blank (ultrahigh purity water) separation. The increase in the concentration of MeOH delivered to the ICP-MS, from 5 to 95% between 0 and 10 min, caused the intensity of the <sup>115</sup>In signal of the internal standard to decrease from  $1.2 \times 10^6$  cps (at 0 min) to  $5.0 \times 10^5$  cps (at 10 min), despite the constant concentration of In in the eluent (Figure 1a). The decline in ICP-MS elemental response occurs as the increasing concentration of MeOH cools the plasma and alters ionization and nebulization efficiency, leading to fewer analyte ions ultimately reaching the detector. Altogether, this causes a steady decrease in detector response as the separation progresses, which is manifested as a decrease in signal intensity (as either peak height or peak area) for a constant concentration of analyte. During the re-equilibration phase of the blank separation (from 12 to 20 min), after the concentration of MeOH returned to 5%, the 115 In signal gradually returned to its initial intensity (Figure 1a). Variable signal is not unique to 115In and was also observed for other metals (Figure S2). Uncorrected, this variation in signal intensity leads to quantitative inaccuracy as the ICP-MS response for a given analyte concentration differs along the solvent gradient. For metal complexes that elute at higher MeOH concentrations, the quantitative error is extreme.

We evaluated the use of an internal standard correction to correct the decrease in ICP-MS response for multiple metals, as this approach has previously been used for LC-ICP-MS quantitation of specific heteroatoms. 20,28-32 However, we found that, on its own, internal standard correction is poorly suited for correcting the solvent effect for quantitation of multiple metals. This is due both to the incompatibility of isotope dilution methods with metals with even isotope distributions (Pb and Cd) and monoisotopic metals (e.g., Mn and Co),<sup>21</sup> as well as to idiosyncratic variation in elemental response with introduction of MeOH to the inductively coupled plasma for methods that normalize to a rare element such as In. By measuring background signal intensities of multiple metals (Mn, Fe, Co, Ni, Cu, Zn, Cd, and Pb) during a blank separation, we observed that the ratio of internal standard (In) to analyte signal intensity varied with solvent conditions and between metal analytes (Figure S2). For Cd and Mn, the analyte to <sup>115</sup>In ratio was 10–20% greater at low MeOH content, while for Fe, Ni, Cu, Zn, and Co, deviation ranged from 30-40% greater at low MeOH (Figure S2). In contrast, the Pb signal decreased by 25% at low MeOH content (Figure S2). These idiosyncratic deviations likely reflect element-specific changes in transport and ionization efficiencies with the increase in MeOH content, rendering internal standard correction unsuitable for accurate multielement correction.

Given the limitations of internal standard correction for multielement LC-ICP-MS quantitation, we implemented a post-column compensation gradient to maintain a constant solvent composition entering the ICP-MS. This approach has been previously used for the quantitation of individual elements (P and Fe), but never (to the best of our knowledge) for simultaneous quantitation of multiple metals. After implementation of the compensation gradient, the <sup>115</sup>In internal standard signal intensity did not deviate significantly across the chromatographic run and remained within 10% of  $5.0 \times 10^5$  cps, demonstrating a steady ICP-MS response throughout the separation (Figure 1b). In comparison, without the compensation gradient the 115In signal intensity decreased by 67% during the separation, from  $1.2 \times 10^6$  cps at the start of the analysis to  $5.0 \times 10^5$  cps at maximum MeOH concentration (Figure 1). In both Figure 1a,b, the <sup>115</sup>In signal intensity reflects a concentration of 2 ppb In after mixing and dilution of the 4 ppb In standard with the LC solvents (Table S5). Thus, while the compensation gradient ensures a constant ICP-MS response, it also decreases ICP-MS sensitivity for fast-eluting compounds.

The accuracy of the compensation gradient method was determined for a mixture of metallophore standards with external matrix-matched multi-elemental calibration. Multielement standard solutions (0 to 200 ppb) were directly infused with the flowrate and matrix of the LC-separated samples, and calibration curves were derived from a linear regression of peak areas (Figure S3). These calibration curves were then used to determine concentrations of each metallophore based on the chromatographic peak area. To correct for instrumental drift across analyses, concentration values were multiplied by a correction factor, calculated as the average <sup>115</sup>In signal intensity of the standards divided the average <sup>115</sup>In signal intensity for each sample. The 115In signal intensity generally declined by less than 1% per hour of operation. This approach yielded the concentrations of cyanocobalamin (retention time = 7.24) and ferrioxamine E (retention time

= 7.55 min) within 6% of their known values, with similar standard deviations (n = 5) (Table S6). Measurement accuracy was reproducible between replicate analyses conducted over a day of continuous instrument operation as well as months apart. As structural differences between metal-DOM complexes have been shown to minimally affect ICP–MS ionization and detection, <sup>19</sup> this method facilitates accurate quantitation of virtually any metal–organic complex, as well as multiple organic-bound metals within chemically distinct DOM fractions, and thus represents a major improvement in quantitative LC–ICP-MS analysis.

The detection limits of the method were calculated from the standard deviation of the peak area of a 2.5 ppb solution of Mn, Ni, Cu, Zn, Cd, and Pb, and a 25 ppb solution of Fe. Eight replicate measurements were used to determine the mean peak area and standard deviations (S) for each metal (Figure S4). The peak area with a 97.5% probability of being greater than zero was calculated as  $t_a \cdot S$ , where  $t_a$  is the test statistic from a one-sided Student t-distribution ( $t_a = 2.306$  for eight replicates). The resulting area was then multiplied by the blank-subtracted mean peak area of the standard solution, divided by the solution concentration (2.5 ppb or 25 ppb) and, finally, multiplied by the molar mass of the metal. Mean metal peak areas in the blank, determined from three replicate measurements of a 1% nitric solution (Figure S4), were used for the blank subtraction. Limits of detection ranged from 0.111 nM for <sup>208</sup>Pb to 1.678 nM for <sup>56</sup>Fe (Table S7).

Effects of Stationary Phase Chemistry on Metal **Recovery.** Incomplete metal recovery during LC-ICP-MS analyses may occur if dissolved metal cations or metal-organic species irreversibly bind to the chromatographic stationary phase. To assess the effects of stationary phase chemistry on metal recovery, we measured the recovery of metals bound to SRNOM and SRFA using four common stationary phases (C18, phenyl, HS F5, and amide), each with different retention mechanisms. We define recovery as the ratio of the concentration of a metal measured by chromatographic separation to the total concentration of the metal measured by direct infusion. SRNOM and SRFA were chosen for these analyses because the chemical heterogeneity and molecular complexity of these DOM mixtures are broadly representative of DOM from a wide range of environments. The SRNOM and SRFA solutions were amended with Co, Ni, Cu, Zn, Cd, and Pb at environmentally relevant concentrations and pH (5.5) such that >97% of each added metal was bound to DOM, as calculated by the NICA-Donnan speciation model (Table S2). The change in solvent polarity during the separation is unlikely to affect metal complexation. Unamended DOM solutions contained minimal concentrations of metals, apart from Fe, which was measured at 3.63 and 1.02 uM Fe in SRNOM and SRFA, respectively (Table S8). After the DOM solutions were amended with metals, Fe recovery decreased 18-23%, likely due to the displacement of organically bound Fe by other metal cations and subsequent adsorption of Fe to vial walls.

We investigated overall trends in metal recovery and separation across stationary phases, individual metals, and DOM mixtures. Recovery varied between metals for different stationary phases, and all stationary phases retained metals to varying extents (Figures 2 and S5 and Tables S9 and S10). On the C18 and amide columns, recoveries of Co, Ni, and Cu were generally higher than recoveries of Zn, Cd, and Pb, and the recovery of Pb was notably low (<60% on C18).

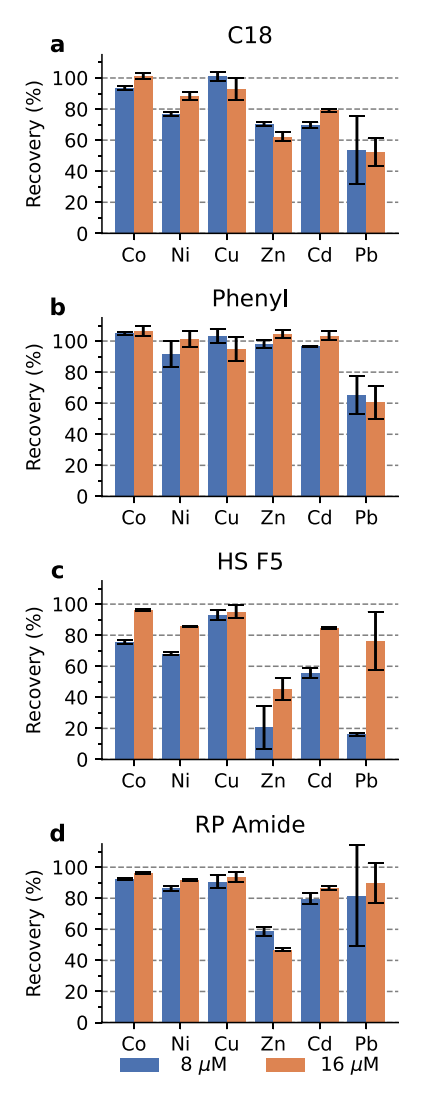


**Figure 2.** Metal recoveries (% total metal injected) for separations of SRNOM amended with 8 and 16  $\mu$ M Co, Ni, Cu, Zn, and Cd and 4 and 8  $\mu$ M Pb, on (a) C18, (b), phenyl, (c) HS F5, and (d) amide stationary phases.

Recoveries were greatest on the phenyl phase and exceeded 90% for all metals except Cu and Pb. Recoveries were typically lowest on the HS F5 phase. Overall, our results indicate that the C18, phenyl, and amide phases are best suited for multi-element analysis of metals complexed with DOM.

Incomplete metal recovery may reflect metal adsorption to residual free silanol groups, although all stationary phases were endcapped to reduce these interactions. Alternatively, strong organic—metal complexes may not elute from the column during the separation. Recovery of Fe generally exceeded 100% in these analyses likely due to leaching of Fe from the stainless-steel column hardware. Thus a C18 column with inert hardware was subsequently used to evaluate Fe recoveries for soil DOM extracts (described below).

Metal recoveries were greater in the SRNOM and SRFA amendments with high metal concentrations than in the amendments with low concentrations (Figures 2 and S5). At higher metal concentrations, partitioning to the stationary phase likely becomes less favorable as metal binding sites on the column particles become saturated. Furthermore, metals which are soft or intermediate Lewis acids (Pb, Cd, and Zn)

appear to have a higher affinity for the stationary phase than hard Lewis acids, as reflected in the lower recoveries of softer metals relative to harder metals (Figures 2 and S5).

Retention and Separation of Organic–Metal Complexes. We next compared how the different stationary phases with distinct retention mechanisms affected the separation of DOM-bound metals into resolvable fractions. We focused our comparison on the C18 and phenyl phases, as retention differed significantly between the two, while retention on the amide phase exhibited intermediate retention characteristics. Overall, we found that compared to the C18 phase, the phenyl phase excelled at separating polar organic—metal compounds. Chromatograms of Cu, Co, and Cd for SRNOM amended with 8  $\mu$ M metals (4  $\mu$ M Pb) on these phases are shown in Figure 3 and for all other metals and stationary phase in

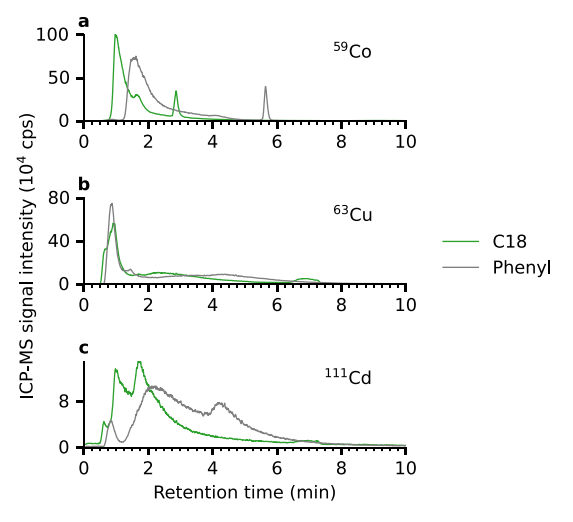


**Figure 3.** Separations of SRNOM amended with 8  $\mu$ M (a) Co, (b) Cu, and (c) Cd on the C18 (green) and phenyl (gray) stationary phases.

Figures S6-S9. Each peak in a chromatogram corresponds to a distinct DOM fraction with similar affinity for the stationary phase. Complexes of the same ligand bound to different bivalent metals generally have similar retention times when separated by reverse phase chromatography. 36,37 The sharp, late-eluting peak in the chromatograms of Co corresponds to the 0.5  $\mu M$  cyanocobalamin internal standard. On the C18 phase, most metal-containing DOM fractions were not well retained and eluted within 2.5 min (Figures 3 and S6-S9). Nonetheless, several distinct fractions were resolved: one from 0.5 to 0.8 min (fraction A, corresponding to the void volume); a second from 0.8 to 1.5 min (fraction B); and a third from 1.5 to 2.0 min (fraction C). Beyond 2.5 min, a narrow feature between 6.4 and 7.6 min was observed in all chromatograms except Co. In addition, a broad feature from approximately 2 to 7 min was observed in the chromatograms of Fe, Cu, and Pb, with a maximum intensity occurring at approximately 3 min. Concentrations of metals complexed to distinct DOM fractions are summarized in Tables S11 and S12.

In general, metal-containing DOM fractions eluted later with the phenyl phase than with the C18 phase. Four distinct fractions were separated on the phenyl phase: one from 0.5 to 1.2 min (fraction E); a second from 1.2 to 2.4 min (fraction F); a third from 1.7 to 3.1 min (fraction G); and a fourth from 3.9 to 5.9 min (fraction H) (Figures 3, S6–S9). These features are noticeably broader than the features in the chromatograms

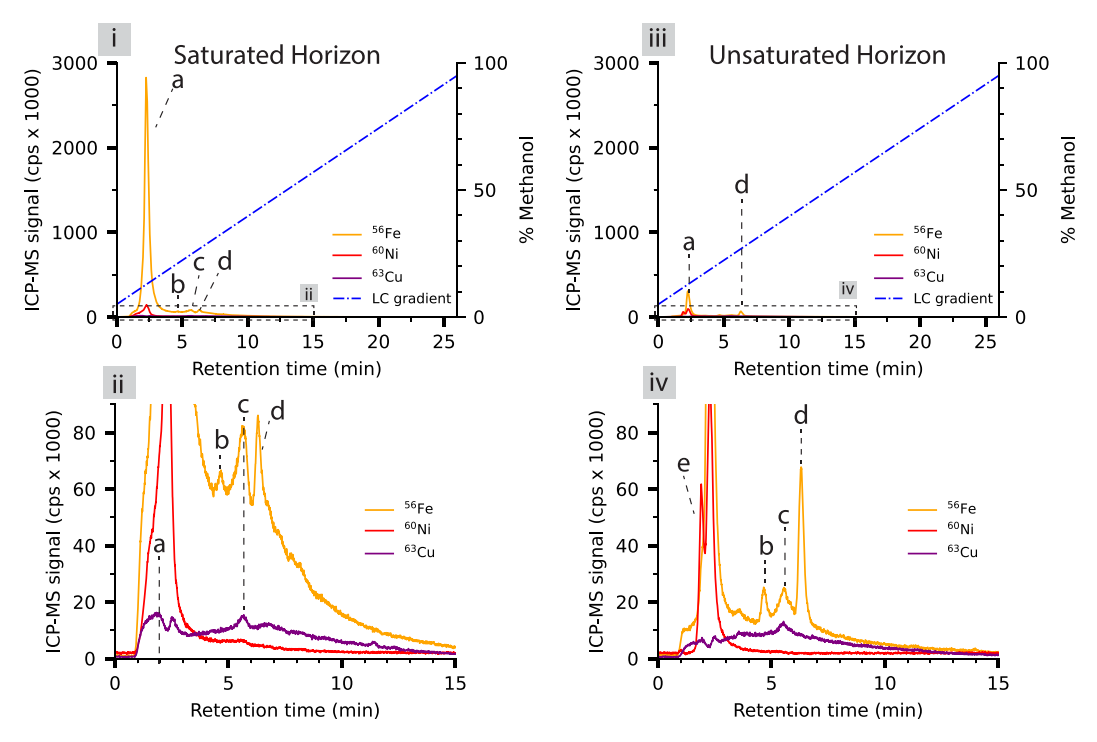


Figure 4. Metal—organic species in water extracts of saturated (left panels) and unsaturated (right panels) soil horizons in the Tims Branch floodplain at the Savannah River Site. The lower (ii, iv) panels show expanded views of the regions demarcated by the dashed boxes (0–15 min) in the upper panels (i, iii).

from the C18 separations. As with the C18 phase, a poorly resolved feature representing a complex mixture is observed in the chromatograms of Fe, Cu, and Pb (Figures 3, S6–S9). However, its maximum intensity is shifted to a later retention on the phenyl phase to approximately 4.5 min. Similarly, the three distinct fractions with Zn and Cd are retained later with the phenyl phase than the C18 phase, resulting in broader features in the chromatograms and thus greater separation of these fractions (Figures 3, S6–S9). Improved resolution of these fractions could be obtained with a longer chromatographic gradient and a longer column.

While LC-ICP-MS does not determine the speciation of organic-metal complexes (per the IUPAC definition<sup>38</sup>) and, further, cannot distinguish inorganic forms of metals from highly polar organic-metal complexes, a quantitative comparison of metals within distinct DOM fractions nonetheless reveals organic-metal speciation that contrasts with NICA-Donnan predictions. The NICA-Donnan model assumes that all metals bind to carboxyl- or phenolic-type sites, which both have a strong preference for binding harder metals, such as Fe and Cu, and a weak preference for softer metals, such as Zn and Cd.<sup>39</sup> However, separations of metal-amended SRNOM reveal the presence of DOM fractions with selectivity for softer metals over harder metals, contradicting the NICA-Donnan model. This is seen clearly in the chromatograms of the phenyl separation, which exhibit a distinct feature between 1.7 and 3.1 min that contains Cd and Zn but not to Fe or Cu, regardless of the concentration of added metal (Figures 3, S6-S9). While additional metal titration experiments are needed to verify that these metals indeed compete for the same organic binding sites, this observation demonstrates the utility of our method for generating new quantitative constraints on metal speciation in complex environmental mixtures.

# Metal Binding Properties of DOM in Floodplain Soils.

We applied our method to quantitively determine metal concentrations within distinct fractions of DOM from different soil redox environments. Soil DOM was extracted from a partially dry horizon (unsaturated horizon, 3800) and a water saturated horizon (saturated horizon, 3801), which differed visibly in texture and color, indicative of contrasting redox conditions (Figure S10). We used a C18 stationary phase with a steel-free flow path and low metal background for separations of these samples, which allowed for accurate quantitation of DOM-bound Fe in addition to other metals. We measured concentrations of Mn, Fe, Co, Ni, Cu, and Zn bound to the extracted DOM and determined metal recovery, which was within 15% of the concentrations measured with direct infusion (Table S13).

The metal-binding properties of DOM differed substantially between the unsaturated and saturated soil horizons, reflecting differences in DOM composition and metal-binding properties across the soil redox environments. Chromatograms of organic complexes of Fe, Cu, and Ni from the horizons are shown in Figure 4. In the unsaturated horizon, 36.5% of total organic Fe was present within a highly polar organic fraction that quickly eluted from the column (peak a, at 2.3 min; Figure 4). Three additional distinct fractions (peaks b, c, and d) cumulatively comprised 8.2% of total organic Fe (Table S14). These fractions were likely phyto- or microbial biomolecules, such as siderophores, used to scavenge Fe in the aerated unsaturated horizon, where inorganic Fe solubility is low. The remainder of the organic-bound Fe (55.3%) appeared as a broad unresolved feature eluting between 3 and 15 min, likely composed of polydisperse organic material derived from degradation processes (Figure 4). Compared to the unsaturated horizon, DOM-bound Fe was 10-fold more concentrated in the saturated horizon, of which 78.4% was present in a highly

polar organic fraction (peak *a*). Fractions *b*, *c*, and *d* comprised less than 0.6% of total organic Fe, respectively. The remainder of organic-bound Fe in the saturated depth was bound to an unresolved complex mixture and comprised 21.1% of total organic Fe (Table S14).

The vast majority of organic Cu—88.4 and 87.3% in the unsaturated and saturated horizons, respectively—was bound to unresolved polydisperse organic material eluting after 3 min, as revealed by the broad Cu peaks (Figure 4). A minor component of Cu (4-10%) was associated with a polar fraction eluting at 1.9 min (peak e) and 2.3 min (peak a) in both horizons (Figure 4 and Table S14). Notably, both horizons contained a small amount of Cu (7.4 and 1.7% for the unsaturated and saturated depths, respectively) associated with a DOM fraction that eluted at 5.6 min, which also appeared to bind Fe (fraction c) (Figure 4 and Table S14).

In contrast to Cu, organic Ni was primarily detected in polar fractions of DOM. In the unsaturated horizon, Ni was predominantly associated with the early eluting peaks at 1.9 min (peak *e*) and 2.3 min (peak *a*), comprising 32.1 and 58.1% of total Ni, respectively, while only 9.8% of total Ni was bound to the unresolved complex mixture eluting after 3 min (Table S14 and Figure 4). In the saturated horizon, 84.6% of total organic Ni was associated with peak *a*, though this estimate likely includes a small contribution from peak *e*, given the shoulder at 1.9 min, while only 14.7% of Ni was bound to the unresolved mixture of polydisperse organic material (Figure 4).

The differences between soil horizons in the distribution and abundance of metals within chemically distinct DOM fractions suggest that redox conditions may be a major determinant of metal-organic speciation in soils. In the saturated horizon, where low oxygen concentrations are expected to inhibit complete mineralization of OM, the greater absolute abundance of unresolved organic Fe and Cu fractions (Figure 4) may reflect a greater concentration of partially degraded DOM relative to the unsaturated horizon. Furthermore, the detection and quantification of at least five distinct components demonstrate how this method can provide information needed to advance metal speciation models beyond the commonly used two-component parameterizations. Future studies are needed to systematically assess the competitive binding of metals to organic ligands from contrasting redox environments.

# CONCLUSIONS

Quantitative detection of dissolved metals within chemically distinct DOM fractions is necessary for predicting the reactivity and solubility—and therefore mobility and uptake—of trace metals in environmental systems. The LC-ICP-MS method described here advances the use of a compensation gradient for the quantitative detection of multiple metals within LC-separated DOM fractions. Using this method, we reveal the effects of stationary phase chemistry on the separation and recovery of organic-bound Mn, Fe, Co, Ni, Cu, Zn, Cd, and Pb. We find that C18, amide, and phenyl chemistries yield highest recoveries, and that the phenyl column excels at separating polar organic-metal fractions. While this method does not reveal the chemical composition of metal-organic species, it can be coupled with high resolution electrospray ionization mass spectrometry for species identification. Additional methods are also needed to characterize the redox state of metals bound to organic ligands, as ICP-MS detects elements regardless of redox state.

Complexation with DOM is an essential control on the biogeochemical cycles of trace metals, yet one that is not well constrained, largely due to the analytical challenge of fractionating and quantifying metal—organic species within the mixture of organic compounds that compose DOM. Our method overcomes these challenges and provides an analytical foundation for advancing our understanding of trace metal biogeochemistry.

# ASSOCIATED CONTENT

# Supporting Information

The Supporting Information is available free of charge at https://pubs.acs.org/doi/10.1021/acs.analchem.3c00696.

Supplemental methods; photo of soil samples; schematic of instrument configuration; plotted ratios of analyte signal intensity to internal standard signal intensity; separations of SRNOM amended with 8  $\mu$ M metals; separations of SRNOM amended with 16  $\mu$ M metals; separations of SRFA amended with 8  $\mu$ M metals; separations of SRFA amended with 16  $\mu$ M metals; amendments to SRNOM and SRFA samples; HPLC operating conditions, ICPMS operating conditions, and standard injection limits of detection; recovery and retention time of chromatographic standards; NICA-Donnan speciation results; total metal concentrations in SRNOM and SRFA samples; metal recovery in SRNOM and SRFA samples; concentrations of recovered metals in SRNOM and SRFA samples; concentrations of metals complexed to distinct ligands groups in SRNOM separated on C18 and phenyl phases; and concentrations and recovery of metals in the Savannah River Site soil samples (PDF)

# AUTHOR INFORMATION

#### **Corresponding Author**

Rene M. Boiteau — College of Earth, Ocean, & Atmospheric Sciences, Oregon State University, Corvallis, Oregon 97331, United States; orcid.org/0000-0002-4127-4417; Email: Rene.Boiteau@oregonstate.edu

#### **Authors**

Christian Dewey — College of Earth, Ocean, & Atmospheric Sciences, Oregon State University, Corvallis, Oregon 97331, United States; Department of Earth System Science, Stanford University, Stanford, California 94305, United States;

orcid.org/0000-0003-1954-8298

Daniel I. Kaplan — Savannah River Ecology Laboratory, University of Georgia, Aiken, South Carolina 29802, United States

Scott Fendorf — Department of Earth System Science, Stanford University, Stanford, California 94305, United States; © orcid.org/0000-0002-9177-1809

Complete contact information is available at: https://pubs.acs.org/10.1021/acs.analchem.3c00696

### **Author Contributions**

The study was designed and implemented by CD and RB, with input from SF. Fieldwork was performed by DK. The manuscript was written by CD with input from all the authors.

#### Notes

The authors declare no competing financial interest.

**Analytical Chemistry** Article pubs.acs.org/ac

# ACKNOWLEDGMENTS

We thank Chris Russo (Oregon State University) for his technical assistance. This work was supported by the U.S. Department of Energy (DOE) (Project Award Numbers DE-SC0020205, DE-AC02-06CH11357, and DE-EM0005228) and the National Science Foundation (CHE-2108340, OCE-1829761).

# REFERENCES

- (1) Gledhill, M.; Buck, K. N. Front Microbiol 2012, 3, 1-17.
- (2) Craven, A. M.; Aiken, G. R.; Ryan, J. N. Environ. Sci. Technol. 2012, 46, 9948-9955.
- (3) Tipping, E. Cation Binding by Humic Substances; Cambridge University Press, 2004.
- (4) Sigg, L. Metals as Water Quality Parameters Role of Speciation and Bioavailability; Elsevier Ltd., 2014; Vol. 4.
- (5) Lehmann, J.; Kleber, M. Nature 2015, 528, 60-68.
- (6) Kinniburgh, D. G.; van Riemsdijk, W. H.; Koopal, L. K.; Borkovec, M.; Benedetti, M. F.; Avena, M. J. Colloids Surf A Physicochem Eng Asp 1999, 151, 147-166.
- (7) De Marco, R.; Clarke, G.; Pejcic, B. Electroanalysis 2007, 19, 1987-2001.
- (8) Tan, W.; Xiong, J.; Li, Y.; Wang, M.; Weng, L.; Koopal, L. K. Colloids Surf A Physicochem Eng Asp 2013, 436, 1152-1158.
- (9) Milne, C. J.; Kinniburgh, D. G.; Tipping, E. Environ. Sci. Technol. 2001, 35, 2049-2059.
- (10) Sedlak, D. L.; Phinney, J. T.; Bedsworth, W. W. Environ. Sci. Technol. 1997, 31, 3010-3016.
- (11) Koopal, L. K.; van Riemsdijk, W. H.; Kinniburgh, D. G. Pure Appl. Chem. 2001, 73, 2005-2016.
- (12) Gustafsson, J. P. J. Colloid Interface Sci. 2001, 244, 102–112.
- (13) Kraemer, S. M.; Duckworth, O. W.; Harrington, J. M.; Schenkeveld, W. D. C. Aquat. Geochem. 2015, 21, 159-195.
- (14) Xu, C.; Zhang, S.; Kaplan, D. I.; Ho, Y.-F.; Schwehr, K. A.; Roberts, K. A.; Chen, H.; DiDonato, N.; Athon, M.; Hatcher, P. G.; Santschi, P. H. Environ. Sci. Technol. 2015, 49, 11458-11467.
- (15) Yu, Q.; Fein, J. B. Environ. Sci. Technol. 2016, 50, 5498-5505.
- (16) Haitzer, M.; Aiken, G. R.; Ryan, J. N. Environ. Sci. Technol. **2002**, *36*, 3564-3570.
- (17) Kaplan, D. I.; Xu, C.; Huang, S.; Lin, Y.; Tolić, N.; Roscioli-Johnson, K. M.; Santschi, P. H.; Jaffé, P. R. Environ. Sci. Technol. 2016,
- (18) Lin, P.; Xu, C.; Kaplan, D. I.; Chen, H.; Yeager, C. M.; Xing, W.; Sun, L.; Schwehr, K. A.; Yamazaki, H.; Saito-Kokubu, Y.; Hatcher, P. G.; Santschi, P. H. Sci. Total Environ. 2019, 678, 409-418.
- (19) Boiteau, R. M.; Fitzsimmons, J. N.; Repeta, D. J.; Boyle, E. A. Anal. Chem. 2013, 85, 4357-4362.
- (20) Lechtenfeld, O. J.; Koch, B. P.; Geibert, W.; Ludwichowski, K. U.; Kattner, G. Anal. Chem. 2011, 83, 8968-8974.
- (21) Boiteau, R. M.; Repeta, D. J. Environ. Sci. Technol. 2022, 56, 3770-3779.
- (22) Sommer, K.; Sperling, M.; Karst, U. Chemosphere 2022, 300,
- (23) Pröfrock, D. Anal. Bioanal. Chem. 2010, 398, 2383-2401.
- (24) Zinn, N.; Hahn, B.; Pipkorn, R.; Schwarzer, D.; Lehmann, W. D. J. Proteome Res. 2009, 8, 4870-4875.
- (25) Quarles, C. D.; MacKe, M.; Michalke, B.; Zischka, H.; Karst, U.; Sullivan, P.; Field, M. P. Metallomics 2020, 12, 1348-1355.
- (26) Pereira Navaza, A.; Ruiz Encinar, J.; Sanz-Medel, A. Angew. Chem., Int. Ed. 2007, 46, 569-571.
- (27) Pereira Navaza, A.; Encinar, J. R.; Ballesteros, A.; González, J. M.; Sanz-Medel, A. Anal. Chem. 2009, 81, 5390-5399.
- (28) Rottmann, L.; Heumann, K. G. Anal. Chem. 1994, 66, 3709-
- (29) Rottmann, L.; Heumann, K. G. Fresenius. J. Anal. Chem. 1994, 350, 221-227.

- (30) Grebe, M.; Pröfrock, D.; Kakuschke, A.; Estella Del Castillo Busto, M.; Montes-Bayón, M.; Sanz-Medel, A.; Broekaert, J. A. C.; Prange, A. J. Anal. At. Spectrom. 2012, 27, 440-448.
- (31) Pan, M.; Lu, Y.; Feng, L.; Zhou, X.; Xiong, J.; Li, H. Anal. Chem. 2022, 94, 11753-11759.
- (32) Heumann, K. G.; Rottmann, L.; Vogl, J. J. Anal. At. Spectrom. 1994, 9, 1351-1355.
- (33) Pröfrock, D.; Prange, A. J Chromatogr A 2009, 1216, 6706-6715.
- (34) Mak, C. K.; Wehe, C. A.; Sperling, M.; Karst, U. J Chromatogr A 2015, 1419, 81-88.
- (35) Langeveld, J.; Bouwman, A. F.; van Hoek, W. J.; Vilmin, L.; Beusen, A. H. W.; Mogollón, J. M.; Middelburg, J. J. SN Appl Sci 2020, 2, 1626.
- (36) Boiteau, R. M.; Till, C. P.; Ruacho, A.; Bundy, R. M.; Hawco, N. J.; McKenna, A. M.; Barbeau, K. A.; Bruland, K. W.; Saito, M. A.; Repeta, D. J. Structural Characterization of Natural Nickel and Copper Binding Ligands along the US GEOTRACES Eastern Pacific Zonal Transect. Front Mar Sci 2016, 3(). DOI: 10.3389/ fmars.2016.00243.
- (37) Boiteau, R. M.; Fansler, S. J.; Farris, Y.; Shaw, J. B.; Koppenaal, D. W.; Pasa-Tolic, L.; Jansson, J. K. Metallomics 2019, 11, 166-175.
- (38) Templeton, D. M.; Ariese, F.; Cornelis, R.; Danielsson, L.-G.; Muntau, H.; van Leeuwen, H. P.; Lobinski, R. Pure Appl. Chem. 2000, 72, 1453-1470.
- (39) Milne, C. J.; Kinniburgh, D. G.; van Riemsdijk, W. H.; Tipping, E. Environ. Sci. Technol. 2003, 37, 958-971.

# **□** Recommended by ACS

**Highly Efficient Photochemical Vapor Generation for** Sensitive Determination of Iridium by Inductively Coupled Plasma Mass Spectrometry

Stanislav Musil, Ralph E. Sturgeon, et al.

FEBRUARY 10, 2023

ANALYTICAL CHEMISTRY

In View of "On-Site" Nuclear Forensics and Assay of Fissile Materials in Sealed Packages by High-Resolution γ-Ray **Spectrometry** 

Satyam Kumar, Rahul Tripathi, et al.

FEBRUARY 01, 2023

ANALYTICAL CHEMISTRY

READ M

Innovative ICP-MS/MS Method To Determine the 135Cs/137Cs **Ratio in Low Activity Environmental Samples** 

Anaelle Magre, Laurent Pourcelot, et al.

APRIL 18, 2023

ANALYTICAL CHEMISTRY

READ C

Speciation Analysis of Selenium Nanoparticles and Inorganic Selenium Species by Dual-Cloud Point Extraction and ICP-**MS Determination** 

Rui Yang, Jingfu Liu, et al.

NOVEMBER 15, 2022

ANALYTICAL CHEMISTRY

RFAD 🗹

Get More Suggestions >